

Evaluation of Die Stress in MEMS Packaging: Experimental and Theoretical Approaches

Satyajit S. Walwadkar and Junghyun Cho

Abstract—The device performance of microelectromechanical system (MEMS) inertial sensors such as accelerometers and gyroscopes is strongly influenced by the stress developed in the silicon die during packaging processes. This is due to the die warpage in the presence of the stress. It has previously been shown that most of the stress is generated during a die-attach process. In this study, we employ both experimental and theoretical approaches to gain a better understanding in a stress development induced during the packaging processes of a small silicon die ($3.5 \times 3.5 \text{ mm}^2$). The former approach is accompanied with an optical profilometer while the latter part by a finite element analysis and an analytical model. A specific emphasis is given to the effects of structural parameters such as the die-attach adhesive thickness and material properties on the stress development. The results from all three approaches show good agreement, in that more compliant and thicker adhesives offer great relief in the stress development, as well as bend the die convex downward from its central location. A stress model proposed from this study not only provides a diagnostic tool for very small stress-sensitive devices, but it will also present a design tool for low-stress MEMS packaging systems.

Index Terms—Adhesives, die-attach, die stress, finite element analysis (FEA), microelectromechanical system (MEMS) packaging, profilometer, simulation, warpage.

I. INTRODUCTION

MICROELECTROMECHANICAL system (MEMS) technology integrates mechanical elements, sensors, actuators, and electronics onto a common substrate by applying so-called microfabrication that is similar to the CMOS fabrications in the microelectronic industry [1]–[3]. Over the years, these devices have become smaller, cheaper, and more functional but require improved reliability. Packaging of the MEMS devices and systems faces additional challenges, as nearly all the MEMS packages are application specific with most of them demanding a direct contact with the environment.

Given that, the silicon die used for the MEMS applications will require more stringent requirements for residual stresses developed during the course of the packaging processes, followed

by thermal cycling [4]. Therefore, it is essential to understand the origin and evolution of the die stress in order to improve the reliability of the MEMS packaging systems. Another concern for MEMS packaging is a long-term drift resulting from slow creep in the die-attach adhesive due to the stresses along with the chemical and mechanical stability of the interfaces formed with the die. It is therefore necessary to choose a proper die-attach adhesive and its curing conditions to optimize the performance of the packaging.

Our previous study has indicated that most of the die stress is developed during curing of the die-attach adhesives [5]. The subsequent packaging processes and thermal cycles added minimal additional stresses to the die. The stress makes the silicon die warped, and more importantly, its development seems to influence the performance of the MEMS sensors [6]. It was therefore suggested that the die stress model be developed to predict the device performance of MEMS sensors and their packaging practices [6].

Given that, the main focus of this work is to examine the stress evolution of the die bonded to the ceramic substrates using the die-attach adhesive. In this experiment, we emulated the actual packaging processes by heat treating the dummy packages with the same thermal history. To assess the stress on these silicon dies, we measured the warpage (curvature; out-of-plane displacement) of the die via an optical profilometer. This tool has a capability to scan a wide range of height information (0.1 nm to 500 μm) [7].

In order to complement the above experimental approach, we also adopted both numerical and analytical modeling. One advantage of the simulation tool is that it can aid to explore a much larger range of parameter space (temperature, materials, geometry, etc.) than is practical experimentally. In addition, the analytical model can be useful to gain a fundamental understanding on the stress development in a simple layered geometry that can represent for our packaging system. The collective information from the theoretical studies will be used to better understand certain experimental observations, and also to steer into the development of the improved packaging system.

II. MEMS PACKAGING PROCEDURE

Packaging techniques for MEMS devices have historically been derived from standard integrated circuits (IC) packaging technologies in order to take advantage of the cost and performance of these existing high volume assembly operations [8]. One of the major challenges in the MEMS manufacturing is thus to develop packaging technologies that meet all the necessary performance and reliability criteria while keeping the cost of the assembly to a minimum [9].

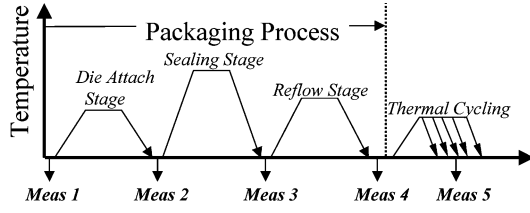
Manuscript received January 3, 2005; revised October 9, 2005. This work was supported by Analog Devices, Inc., New York State, and the Integrated Electronics Engineering Center (IEEC), State University of New York at Binghamton. This work was recommended for publication by Associate Editor P. Lall upon evaluation of the reviewers' comments.

S. S. Walwadkar was with the Department of Mechanical Engineering, Integrated Electronics Engineering Center, State University of New York at Binghamton, Binghamton, NY 13902-6000 USA and is now with the Systems Manufacturing Analysis Center (SMAC), Intel, Hillsboro, OR 97124 USA.

J. Cho is with the Department of Mechanical Engineering, Integrated Electronics Engineering Center, State University of New York at Binghamton, Binghamton, NY 13902-6000 USA (e-mail: jcho@binghamton.edu).

Color versions of Table I and Figs. 2–10 are available online at <http://ieeexplore.org>.

Digital Object Identifier 10.1109/TCAPT.2006.885931



Packaging Processes	Experimental Conditions
Die attach	Silver Glass cured at 355°C. Polyimide cured at 100°C for 30 min and 200°C for 30 min.
Top lid Sealing Process	Peak temp of 340°C
Reflow Process	Peak temp of 240°C

Fig. 1. Standard packaging processes followed by thermal cycles and corresponding heat treatment conditions used in this study for the stress measurements.

In this work, dummy silicon dies ($3.5 \times 3.5 \text{ mm}^2$) were assembled onto the ceramic substrates with the help of two different die-attach adhesives (silver glass, polyimide). The silver glass adhesive has a higher modulus and a higher coefficient of thermal expansion (CTE) than the polyimide counterpart. After attaching the silicon die to the substrate, this assembly was passed through a series of heat treatments that emulate the actual MEMS packaging processes as shown in Fig. 1. In order to measure thickness of the die-attach adhesive layer between the silicon and the substrate, optical microscope (OM) and scanning electron microscope (SEM) were utilized. Three different techniques including a numerical modeling, an analytical calculation, and an optical measurement were explored in this work to evaluate the stress development in these packaging processes.

III. STRESS MEASUREMENTS

A. Optical Profilometer

In an attempt to assess the stress in a silicon die, a noncontact, optical profilometer (WYKO RST Plus System, Tucson, AZ) was used to measure warpage of the die by tracing its surface profile. This instrument uses interferometric technique along with the digital signal processing algorithms to produce accurate, repeatable three-dimensional (3-D) surface profiles. We used scanning white light interferometry (SWLI), in which an incoming light is split onto an internal reference surface and a silicon die surface. After reflection, the light beams recombine inside the interferometer, thereby undergoing constructive and destructive interference and producing light and dark fringe patterns [6].

Bare silicon dies, cut from the silicon wafers, were assembled in the packages, treated for the aforementioned heat treatments, and measured for die warpage using the profilometer. The maximum deflection was measured from the topmost point of the surface profile. All the measurements were performed at room temperature, and each sample was measured at least three times nonconsecutively. The stresses developed in the die were determined from the surface profiles by assuming the die as a thin

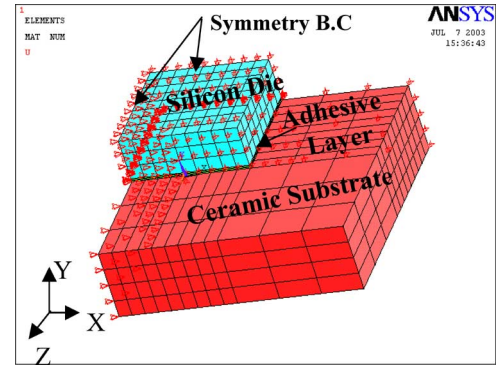


Fig. 2. Geometry of the quarter symmetry 3-D model used in the simulation.

plate bent by moments uniformly distributed along the edges, according to the theory of elasticity

$$\sigma_x = \frac{Et(1/R_x + \nu/R_y)}{(1 - \nu^2)}$$

$$\sigma_y = \frac{Et(1/R_y + \nu/R_x)}{(1 - \nu^2)} \quad (1)$$

where E is Young's modulus, ν is Poisson ratio, t is a half of the thickness of the die, and R_x and R_y are the radius of curvature in the x - and y -direction, respectively [10], [11]. This stress analysis can only be valid if the shear stresses are much smaller than the bending stresses.

B. Simulation

In this study, we improved our simulation model by incorporating 3-D implementation from the previously developed two-dimensional (2-D) model [5]. This 3-D model was constructed using the ANSYS finite-element analysis (FEA) software package [12]. Only a quarter of the assembled package was modeled using the symmetry boundary condition: along the line of symmetry, displacements in x and z directions are confined (i.e., $U_x = 0$ and $U_z = 0$); at the bottom most node, no displacements occur in all three directions (i.e., $U_x = 0$, $U_y = 0$, $U_z = 0$) to prevent a rigid body motion (Fig. 2). The material properties for silicon, ceramic and the adhesive layer were assumed to be linear-elastic (Table I). The assumption of linear elastic properties can work well for the silicon die and the ceramic substrate, but are less realistic for the adhesive layer due to the existence of the glass transition temperature (T_g).

Therefore, the other improvement that was adopted here was to choose "temperature-dependent" nature of the adhesive materials. For simplicity, we implemented it by considering a viscous effect for the die-attach adhesive layer above T_g . In this temperature range, the silver glass will exhibit a viscous flow while the polymer adhesives such as polyimide will exhibit a viscoelastic flow. Although it is not exactly capturing the temperature dependence of the adhesive, this assumption will enforce no stress development in the silicon die due to the fluidic adhesives above T_g , thereby providing a better comparison with the experimental counterparts. The thermal loads for the simulation were thus chosen between room temperature (27 °C) and T_g for the individual adhesive types (silver glass $T_g = 155$ °C;

TABLE I
MATERIALS PROPERTIES AND GEOMETRY USED IN THE SIMULATION [17]

Materials	E (GPa)	Poisson's ratio	CTE (ppm/°C)	Thickness (mm)	Width (mm)
Si die	190	0.28	3.1	0.675	3.5
Ceramic substrate	386	0.28	8.6	1.04	7.3
Die-attach adhesive:					
Silver glass	11.5	0.35	16	0.05	3.5
Polyimide	2.47	0.40	13	0.05	3.5

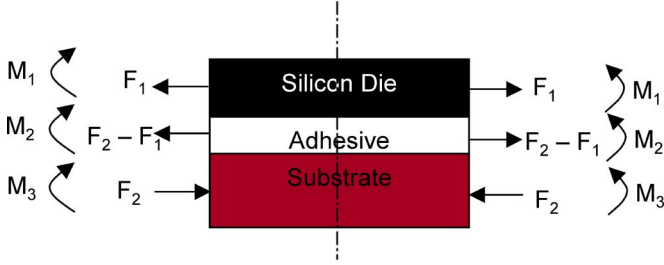


Fig. 3. Simple trilayer [Si (1)-adhesive (2)-substrate (3)] assembly used for analytical modeling. (F: in-plane force, M: bending moment).

polyimide $T_g = 150$ °C) regardless of the actual temperature profile.

Our previous studies have indicated that most of the stresses result from the adhesive curing during the die-attach process [5], [6]. The numerical modeling considers a cooling cycle from the elevated temperatures to room temperature. The deflection in the silicon die was assessed by measuring the difference in the displacement values of the two nodes on the top.

C. Analytical Model

There have been several models developed to understand the thermal stress developed in the bilayer and trilayer systems due to the CTE mismatch [13]–[17]. In this study, a simple analytical model based on the Suhir's work [18] was taken into consideration to check the validity of numerical and experimental results. The structure (trilayer) in question is assumed to be manufactured at an elevated temperature and subsequently cooled. Fig. 3 shows the configurations of the trilayer structure. A change of temperature ΔT induces forces and moments in the layers, which upon cooling produce curvature in the assembly. This is due to the interfacial compatibility of displacements that are required at the cooled temperature from the stress-free die-attach temperatures.

The deflection of the silicon therefore depends on the thickness and material properties of each layer, as well as the CTE mismatch. Thermal loads were modified to incorporate the viscous effects of the adhesive, as described in the simulation work. In the Suhir's model, the deflection set up for such a trilayer assembly is given by

$$w_{\max} = \frac{t l^2 \Delta \alpha \Delta T}{4 \lambda D} \left[1 - 2 \frac{\cosh(kl) - 1}{(kl)^2 \cosh(kl)} \right] \quad (2)$$

where w_{\max} is the maximum bow of the assembled package, t is the thickness of the package ($t = T_1 + T_2 + T_3 \approx T_1 + T_3$),

l is the length of the package, $\Delta \alpha$ is the thermal expansion mismatch between the substrate and die ($= \alpha_3 - \alpha_1$), ΔT is the temperature difference, k is the eigenvalue (parameter of assembly stiffness), and λ is the axial compliance of the assembly ($\lambda = \lambda_1 + \lambda_3 + \lambda_{13} = (1 - \nu_1)/E_1 T_1 + (1 - \nu_3)/E_3 T_3 + t^2/4D$), where D is the total flexural rigidity of the assembly ($D \approx D_1 + D_3 = E_1 T_1/12(1 - \nu_1^2) + E_3 T_3/12(1 - \nu_3^2)$) and ν is the Poisson's ratio.

For large assemblies/stiff attachments, the above formula for deflection simply follows deflection behavior obtained by Timoshenko as given by [19]

$$w_{\max} = \frac{t l^2 \Delta \alpha \Delta T}{4 \lambda D}. \quad (3)$$

IV. RESULTS AND DISCUSSION

Fig. 4 shows 3-D surface profiles of the silicon die assembled to the ceramic substrate. As seen here, a dome-shaped surface profile was found, indicating the die warpage resulting from a compressive stress. The profile was acquired after the test die was attached to the substrate, and heat treated at the temperature that is used for an actual sealing process for the top lid of the ceramic package. In order to estimate the warpage (curvature), a line profile across both x-direction and y-direction was drawn as shown in Fig. 4(b).

The die warpage due to the stress development in the assembly is also visible in the numerical modeling result when the packaging assembly is subjected to a thermal load, ΔT ($T_g = 155$ °C to room temperature) (Fig. 5). A similar convex-down surface profile of the Si die can be seen in Fig. 5(b) because of the CTE mismatch between the Si die and the substrate. It does not seem that the CTE of the adhesive layer has a significant role on the stress development of the die, due to its small thickness compared to that of the die and the substrate as well as its lower modulus.

Fig. 6 shows a comparison between the deflection values obtained by using three different methodologies (discussed above) for the silver glass and polyimide adhesives after the packages were passed through up to the heat treatment equivalent to the reflow stage. It is seen that the silver glass adhesive produces more deflection in the silicon die as compared to the polyimide adhesive. The structure initially has no stress developed, when the bonding medium is in the liquid state. Upon cooling, the bonding medium becomes solidified and stress is induced due to a CTE mismatch among the die, the die-attach, and the substrate, and also due to the shrinkage of the die-attach adhesive during curing. The polyimide adhesive being compliant showed

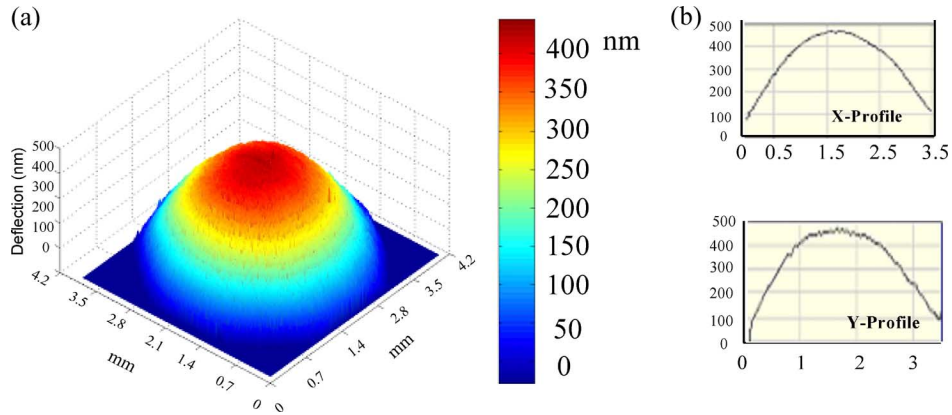


Fig. 4. Three-dimensional surface profile of the silicon die showing (a) uniform deflection (b) line profile across both x and y direction indicating warpage of the silicon die.

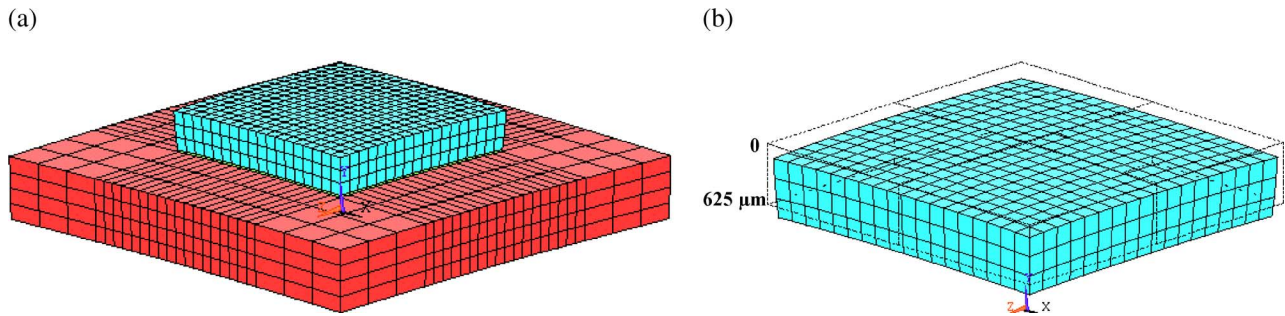


Fig. 5. Simulation result from the package assembled with the silver glass adhesive (0.05-mm thick): (a) whole package warpage and (b) Si die warpage.

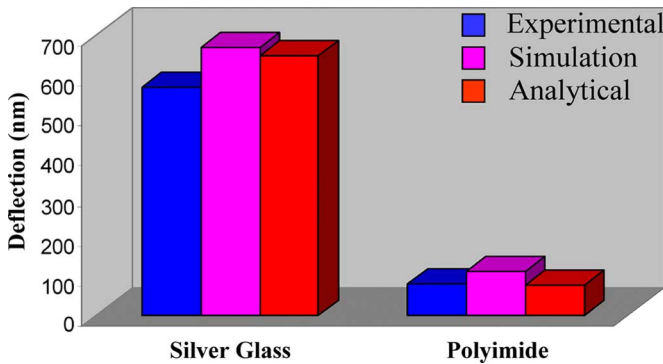


Fig. 6. Deflections obtained for the packages assembled with the 0.05-mm thick silver glass and the 0.05-mm thick polyimide adhesives using three different methods (experimental, simulation, and analytical model).

lower stress levels, suggesting that it accommodate the stress more effectively as a buffer layer. However, for stiffer materials like the silver glass, much of the stresses are transferred to the silicon die, thus increasing its warpage.

Although some discrepancies in the magnitude of the deflection were found, there existed a good correlation among three methodologies. In particular, the numerical simulation was much improved as compared to the previous studies using a 2-D simulation and temperature-independent materials properties, which were not accurate enough to predict the experimental stress values [5]. Given that, we further investigated the stress development using the theoretical approaches. In

these approaches, we can easily isolate one variable at a time to understand better its effect on the stress development.

A. Effect of Thickness of Die-Attach Adhesives

The thickness of the die-attach adhesive plays a major role in reducing the die stress since the adhesives can accommodate the stresses developed due to the CTE mismatch between the silicon die and the ceramic substrate. Since the adhesives shrink during curing, it must also be minimized for better performance of the die-attach adhesives. In addition, actual packaging processes result in a significant variation in thickness of the adhesives. Therefore, it is of great importance to know about the thickness effects.

Fig. 7 shows the thickness effects on the stress development in the silicon die assembled with two different die-attach adhesives. For both systems, no delamination was observed at the interfaces even with large deflections. The simulation and analytical modeling results are compared with the experimental warpage measurements. For direct comparison, the stress values were evaluated using (1) from the deflections measured or calculated assuming only bending stresses under uniform edge moments. It is shown that the stress linearly decreases as the thickness increases for the packages assembled with a silver glass adhesive. The error bars represent for the x - and y -values of the deflection averaged from three measurements. There are possibly two reasons for such thickness-dependent behavior: 1) increased standoff distance between the silicon die and the substrate, resulting in decoupling the Si die from the substrate and 2) more

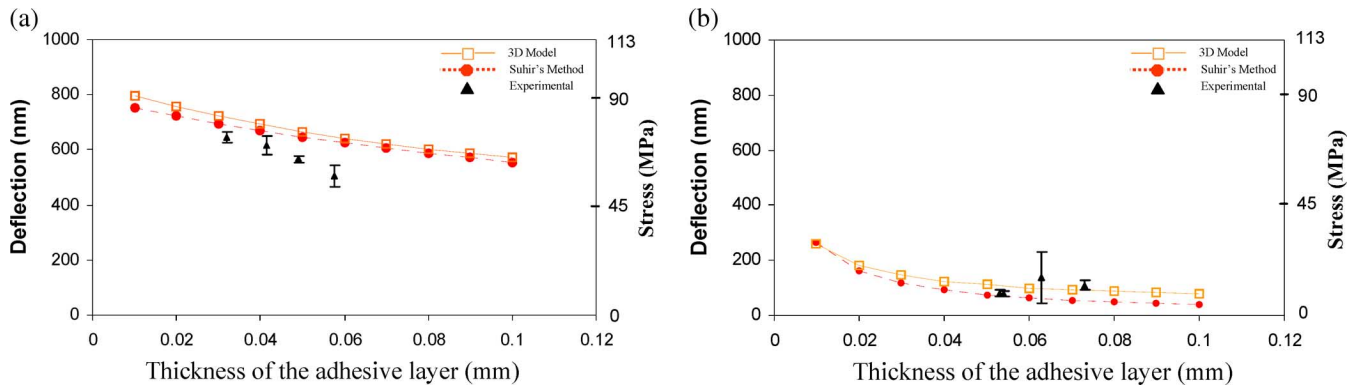


Fig. 7. Effect of the die-attach adhesive thickness on the deflection (i.e., stress) developed in the silicon die assembled with (a) the silver glass adhesives and (b) the polyimide adhesives.

effective buffer layer to accommodate the CTE mismatch between Si and the substrate [20]–[22]. In addition, experimental values are deviated further as the adhesive becomes thicker.

On the other hand, the die deflection values become constant beyond certain thicknesses (0.08-mm in this case) for the polyimide adhesive. With the limited data from the experiments, there was no significant thickness dependence for this adhesive. It indicates that thicker adhesive layers will not produce any more effect once it reaches the critical value unlike the silver glass adhesive that shows a continuous decrease in the thickness range tested. It suggests that the silver glass adhesive have a further reduction in the stress development by simply making it thicker, and that it require a thicker layer to reach the constant stress.

This observation can provide an important manufacturing variable for packaging processes as the thickness of the adhesive can be easily controlled, and affect the device performance via the stress generation. Again, the magnitude of the deflection obtained with simulation and analytical modeling show a good correlation with the experimental results for both the silver glass and polyimide adhesives.

Further, the stress distribution at the top surface of silicon die was examined through numerical simulation. The displacement in the Si die gradually decreases with an increasing distance from the center of the die (Fig. 8). As before, the displacement is smaller for the polyimide adhesives. Interestingly, the stress at the top surface of the silicon die is maximum (tensile) near the edge of the die, which indicates that the silicon die will be bent more near the edge rather than near the center of the die. This “edge” effect can be attributed to more coupling between Si and the substrate as the thickness of the adhesive layer is small as compared to the other two layers, and thus become more pronounced with the stiffer adhesive. For example, as the modulus of the adhesive increases (i.e., the silver glass case), the maximum stress location moves further toward the edge of the die as shown in the 3-D stress contour plot Fig. 8(a). As a result, if more compliant adhesive is used, the stress will ultimately be at its maximum near the center of the die, resulting in uniform bending from the center of the die. In fact, the silicone adhesive (modulus of 10 MPa) confirmed this trend [17].

The stress distribution also changes with the thickness of the die-attach adhesives. As shown in Fig. 9, as the thickness of the

adhesive layer increases, the stress profile becomes more uniform bending from the center of the die (that is, less edge effect). A possible explanation for this behavior is that, with an increase in the thickness of the adhesive layer, the substrate and the die gets decoupled each other and the thermal stresses in the silicon die are more influenced by the material properties and the configurations of the adhesive layer. The package with the silver glass needs a thicker adhesive layer to have uniform stress distribution than that with the polyimide. Thus, it seems harder to decouple between Si and the substrate when the adhesive layer becomes stiff.

It again has an important implication for the manufacturing aspects from the stress development in the silicon die. Since the MEMS structures and components are fabricated at the top surface of the silicon die, it will be much beneficial to place the stress-sensitive structures and components close to the low stress locations depending on the adhesive used and its thickness.

B. Effect of Material Properties

As shown before, the packages assembled with different adhesives behave differently in terms of the stress development and the dependence on the thickness. In order to characterize the effect of material properties such as Young’s modulus and CTE, we have compared the deflection by adjusting these values. While we only have two adhesives from the experiment, the simulation can deal with much wider range of Young’s modulus and CTE. In addition, it can isolate its effect by keeping the rest of the other variables constant. Therefore, it was attempted to simulate the effects from the CTE and Young’s modulus.

As shown in Fig. 10, Young’s modulus has a significant impact on the stress development while the CTE has little impact on this. For example, by reducing the modulus value for the adhesive layer, the deflection value decreases substantially. Therefore, it is clear that the adhesives having lower Young’s modulus will be a good choice for reducing the stresses in MEMS packages. On the other hand, since both silicon and ceramic layers are stiffer and thicker than the adhesive layer, the CTE effect does not become important with the range tested in this study.

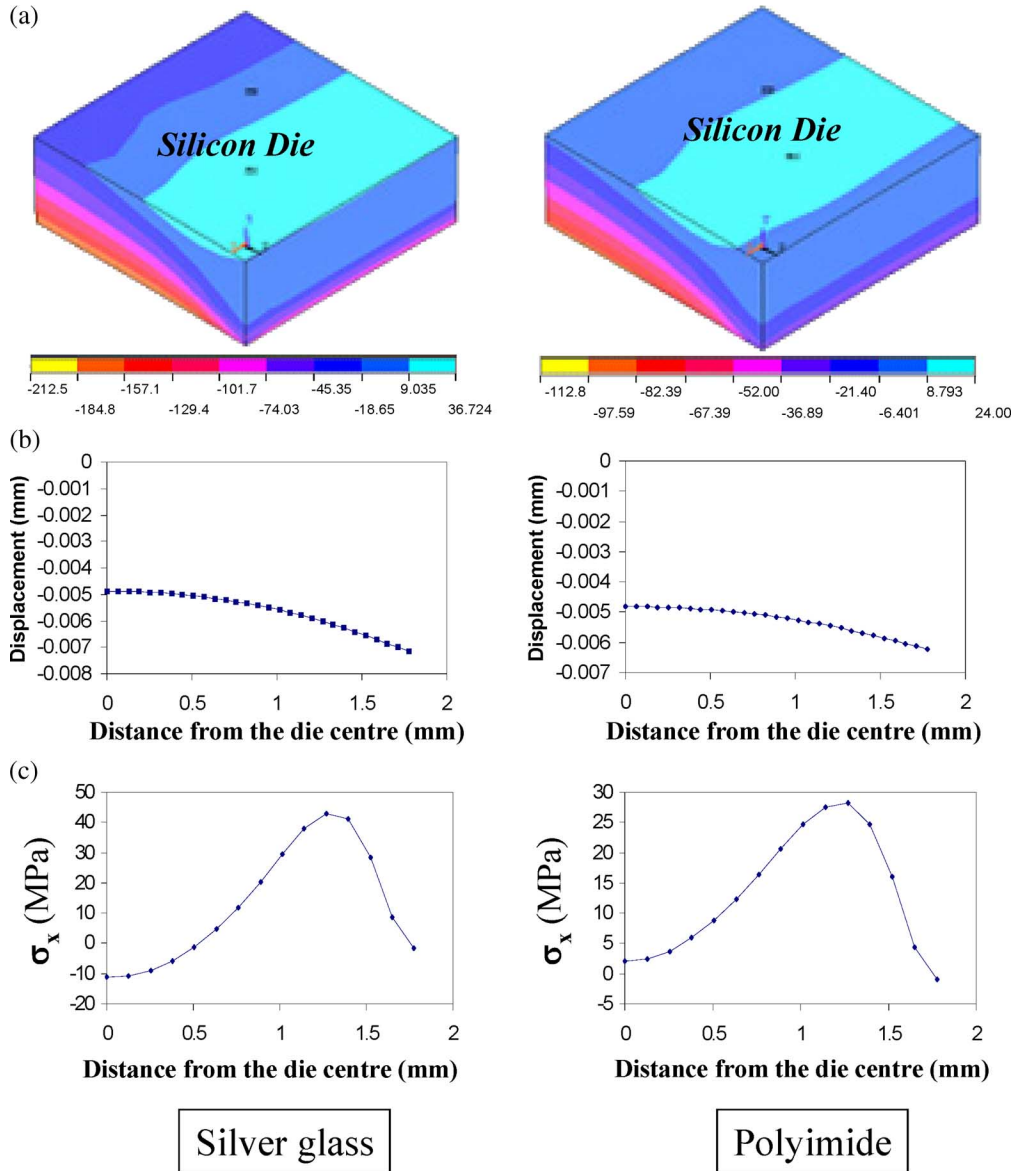


Fig. 8. Simulation result showing (a) stress contour (scale bar in MPa), (b) displacement, and (c) stress in the x -direction, observed along the top surface of the silicon die for two different adhesive types. Both adhesives have a thickness of 0.05 mm. (left: silver glass adhesive, right: polyimide adhesive).

C. Comparison Among Experiments and Theoretical Approaches

Although several phenomena regarding the die stress evolution and distribution have been reproduced by the theoretical models, it is also appropriate to acknowledge some of their limitations here. These theoretical approaches are based on certain basic assumptions that perfect bonding exists among the three layers, and that the packaged assembly has uniform temperature distribution across the whole layers. In addition, the deformation of these layers follows linear elastic behavior. Neither plastic deformation nor stress relaxation is considered in the modeling work, thereby strictly limiting its application to the cooling from the elevated temperature, or vice versa. One exception is that the adhesive layer is assumed to impose no stress on the Si die above the glass transition temperature due to its viscous nature. Theoretical models are also based on the perfect geometry while in actual packages, there exists a sample-to-sample variation in

terms of thickness, die tilting, and non-uniformity in the adhesive composition and structure [17].

In this context, there is a room for this simulation to be further developed into more realistic model, wherein the stress relaxation mechanism is possible during the course of several heating and cooling cycles, and the “true” temperature-dependent material properties are implemented. This will in turn provide a means of monitoring temporal evolution of the stress during a series of thermal loads during the packaging processes and device operation conditions.

Despite the limitations mentioned above, our models worked well to reproduce the experimental stress values. This is partly due to the fact that most of the stresses are generated during die-attach process as described in the Introduction. In fact, by adopting the 3-D simulation and viscous nature of the adhesive above T_g from the previous studies, the numerical modeling work was improved significantly [5]. The simulation indeed highlighted the influence of the die-attach materials on the stresses developed in

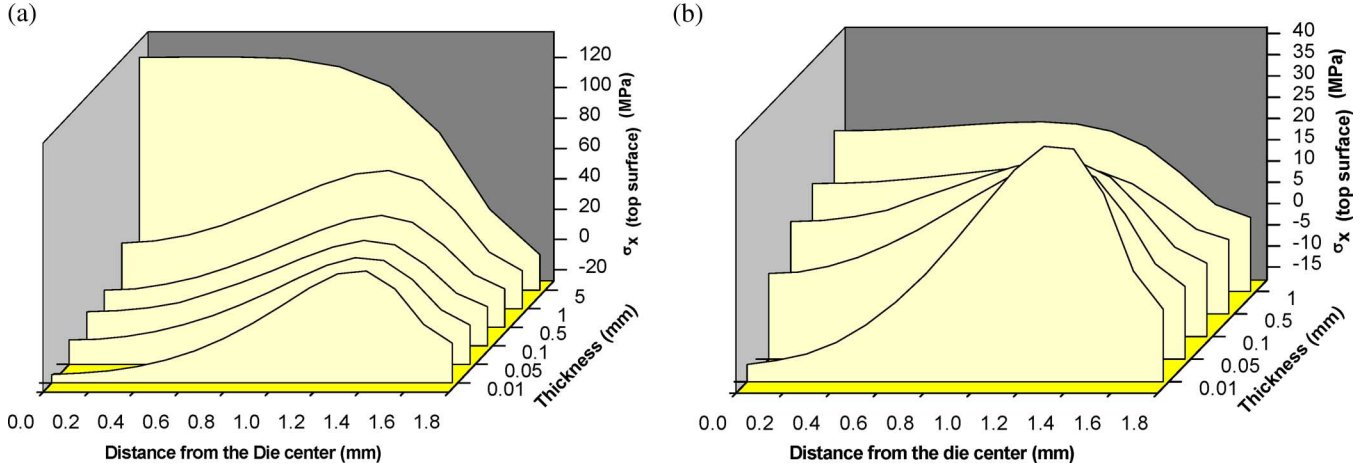


Fig. 9. Stress distribution observed along the top surface of the silicon die at different die-attach thicknesses for (a) silver glass and (b) polyimide through numerical simulation.

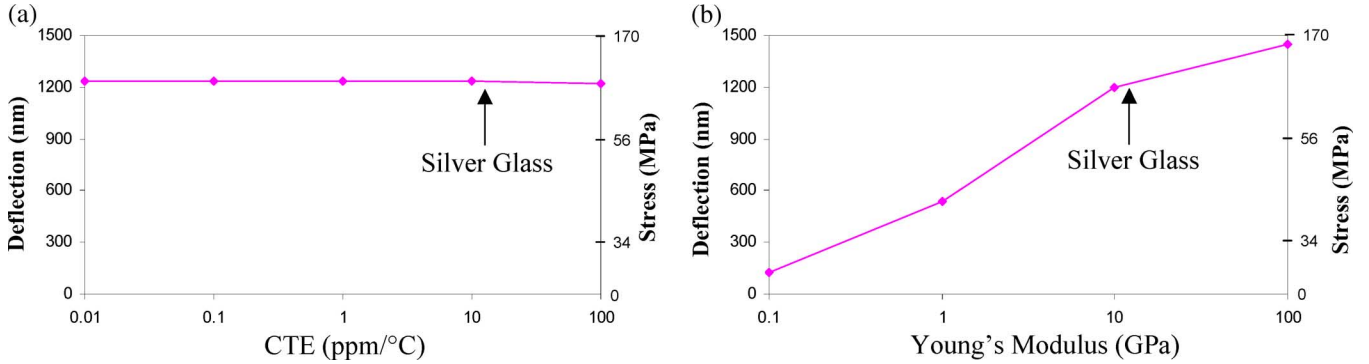


Fig. 10. Effect of materials properties of the adhesive layer on warpage set up in the silicon die: (a) CTE and (b) young's modulus. The arrow mark indicates the property of the silver glass adhesive.

the packaging. Given that, it will have a significant advantage over the experimental approaches as the die-attach parameters can be systematically varied to see their effect. Experimentally, it will involve exhaustive testing to avoid the manufacturing variation and to monitor numerous parameters.

Finally, it is of interest to explore the implications of these results for the stress development in MEMS packaging. From this study, it is shown that the stress development depends mostly on the die-attach processes and materials, as well as the adjoining material geometries. Depending on which types of the adhesives are adopted, one can use the stress model to choose the optimum packaging geometry and manufacturing parameters. For example, the prediction of the thickness needed for the specific stress distribution from the theoretical models can be quite useful due to its simplicity. Therefore, to the extent that the stress controls the MEMS device performance, as exemplified by the previous studies [6], finding a way to tailor the stress development and distribution will likely play a key role in manufacturing of these devices. One must, however, consider other factors such as interfacial adhesion and strength of the adhesive layer while choosing the die-attach adhesives for a low die stress development to optimize overall performance in MEMS packaging.

V. CONCLUSION

In this study, we explored the effect of the die-attach parameters in MEMS packaging to understand the die stress develop-

ment in MEMS devices. For this purpose, three different techniques (experimental, numerical, analytical) have been used to measure the deflection of the silicon dies assembled with two different die-attach adhesives. A good agreement was found among three different techniques (experimental, numerical, analytical). In particular, the noncontact, optical profilometer successfully measure warpage (curvature) occurred due to the stress in a small Si die ($3.5 \times 3.5 \text{ mm}^2$).

Between the two different adhesives used, the polyimide adhesive exhibits less stress development in the silicon die than does the silver glass due to its lower modulus. It can act as a more effective buffer layer when sandwiched between the die and the substrate. Also our results indicate that the warpage (i.e., stress) in the silicon die can be further minimized by using relatively thicker adhesive layers with a possible saturation value beyond which its effect will be no longer significant. These modulus and thickness parameters, of course, must be balanced with other factors in overall manufacturing designs and processes. The stress distribution at the top surface of the silicon die can also depend on those two parameters of the adhesives. Importantly, the numerical simulation of the die stress in MEMS packaging, validated by both experiment and analytical model, can work as an invaluable tool to monitor the performance of the MEMS devices, as well as to be used for the design of low-stress MEMS packaging systems.

ACKNOWLEDGMENT

The authors wish to thank Dr. B. Sammakia and Dr. H. Ackler, SUNY Binghamton, and Dr. L. E. Felton and P.W. Farrell, Analog Devices, for helpful discussions.

REFERENCES

- [1] S. M. Spearing, "Materials issues in micro-mechanical systems (MEMS)," *Acta Mater.*, vol. 48, pp. 179–196, 2000.
- [2] J. J. Sniegowski and M. P. de Boer, "IC-compatible polysilicon surface micro-machining," *Annu. Rev. Mater. Sci.*, vol. 30, pp. 299–333, 2000.
- [3] L. Cao, S. Mantell, and D. Polla, "Design and simulation of an implantable medical drug delivery system using micromechanical systems technology," *Sens. Act. A*, vol. 94, no. 1–2, pp. 117–125, 2001.
- [4] P. H. Tsao and A. S. Voloshin, "Manufacturing stresses in the die due to the die attach process," *IEEE Trans. Comp., Packag., Manufact. Technol. A*, vol. 18, no. 1, pp. 201–205, Mar. 1995.
- [5] S. Walwadkar, P. W. Farrell, L. E. Felton, and J. Cho, "Effect of die-attach adhesives on the stress evolution in MEMS packaging," in *Proc. 36th Int. Symp. Microelectron. (IMAPS'03)*, Boston, MA, Nov. 2003, pp. 847–852.
- [6] S. Walwadkar, J. Cho, P. W. Farrell, and L. E. Felton, "Tailoring of stress development in MEMS packaging systems," in *Proc. NEMS MEMS Mol. Mach.*, Warrendale, PA, 2003, vol. 741, pp. 139–144.
- [7] B. Bowe and V. Toal, "White light interferometric surface profiler," *Opt. Eng.*, vol. 37, no. 6, pp. 1796–1799, 1998.
- [8] M. L. Kniffin and M. Shah, *Int. J. Microcirc. Electron. Packag.*, vol. 19, no. 1, pp. 75–86, 1996.
- [9] A. Morrissey *et al.*, "Selection of materials for reduced stress packaging of a microsystem," *Sens. Actuators*, vol. 74, pp. 178–181, 1999.
- [10] J. W. Dally and W. F. Riley, *Experimental Stress Analysis*, 3rd ed. New York: McGraw-Hill, 1991.
- [11] E. E. Sechler, *Elasticity in Engineering*. New York: Dover, 1968.
- [12] "ANSYS Theory Manual," ANSYS, Inc., Houston, PA, 2001.
- [13] E. Suhir, "An approximate analysis of stresses in multilayered elastic thin films," *J. Appl. Mech.*, vol. 55, pp. 143–148, 1998.
- [14] W. T. Chen and C. W. Nelson, "Thermal stresses in bonded joints," *IBM J. Res. Develop.*, vol. 23, no. 2, pp. 179–188, 1979.
- [15] T. Y. Pan and Y. H. Pao, "Deformation in multilayered stacked assemblies," *J. Electron. Packag.*, vol. 112, pp. 30–34, 1990.
- [16] S. B. Park *et al.*, "Predictive model for optimized design parameters in flip chip packages," in *Proc. Int. Soc. Conf. Thermal Phenom.*, 2004, pp. 458–464.
- [17] S. S. Walwadkar, "Tailoring of Stress Development in MEMS Packages," M.S. thesis, State Univ. New York, Binghamton, 2004.
- [18] E. Suhir, "Die attachment design and its influence on thermal stresses in the die and the attachment," in *Proc. IEEE/Electron. Ind. Assoc. (EIA) 37th Electron. Comp. Conf.*, 1987, pp. 133–138.
- [19] S. Timoshenko, "Analysis of Bi-metal thermostats," *J. Opt. Soc. Amer.*, vol. 11, pp. 233–255, 1925.
- [20] J. C. Bolger, "Polyimide die attach adhesive for LSI ceramic packages," in *Proc. 14th Nat. SAMPE Tech. Conf.*, 1982, vol. 1, pp. 257–266.
- [21] J. C. Bolger and C. T. Mooney, "Failure mechanisms for epoxy die attach adhesives in plastic encapsulated I.C.'s," in *Proc. Electron. Comp. Conf.*, 1983, pp. 227–231.
- [22] F. K. Moghdam, "Development of adhesive die attach technology in Cerdip packages," in *Proc. Int. Microelectron. Symp.*, 1983, pp. 79–87.



Satyajit S. Walwadkar received the M.S. degree in mechanical engineering from the State University of New York at Binghamton in 2005. His M.S. thesis work was on stress evolution in MEMS/RF devices during the packaging process.

He is currently a Failure Analysis Engineer with the Systems Manufacturing Analysis Center (SMAC), Intel Corporation, Hillsboro, OR, and his current work includes material and failure analysis to enhance processing and reliability of electronic components. Prior to joining Intel he was a Research

Assistant with the Integrated Electronics and Engineering Center (IEEC), Binghamton, NY.

Mr. Walwadkar received the Best Poster Award at the IMAPS Optoelectronics Device and Packaging and Materials in 2003.



Junghyun Cho received the B.S. degree in metallurgical engineering from Yonsei University, Seoul, Korea, in 1991, the M.S. degree in materials science and engineering from Northwestern University, Evanston, IL, in 1993, and the Ph.D. degree in materials science and engineering from Lehigh University, Bethlehem, PA, in 1999.

Before starting his graduate studies, he was with the Samsung Semiconductor R&D Center, Kihung, Korea. He joined the State University of New York (SUNY) at Binghamton as an Assistant Professor with the Department of Mechanical Engineering in 2001 after finishing a Postdoctoral Research Appointment at the University of California, Santa Barbara. His research interests are in the area of thin films and coatings for their structure/property relationships, microstructural design, and mechanical properties at nano- and micro-scales.

Dr. Cho received the NYSTAR Technology Transfer Initiative Program Award in 2006, the SUNY Chancellor's Promising Inventor Award in 2003, and the Rowland B. Snow Award from the American Ceramic Society Meeting in 1999.